mRNA encoding the β-subunit of the mitochondrial F_1-ATPase complex is a localized mRNA in rat hepatocytes

Gustavo EGEA*, José M. IZQUIERDO, Javier RICART, Carmen SAN MARTÍN† and José M. CUEZVA‡

Departamento de Biología Molecular, Centro de Biología Molecular 'Severo Ochoa', Universidad Autónoma de Madrid, Consejo Superior de Investigaciones Científicas, Universidad Autónoma de Madrid, 28049 Madrid, Spain

Subcellular mRNA localization has emerged as a mechanism for regulation of gene expression and protein-sorting pathways. Here we describe the different cytoplasmic presentation in rat hepatocytes of two nuclear mRNA species encoding subunits α and β of the mitochondrial F_1-ATPase complex. α-F_1-ATPase mRNA is dispersed and scattered in the cytoplasm. In contrast, β-F_1-ATPase mRNA appears in rounded electron-dense clusters, often in close proximity to mitochondria. Hybridization experiments with β_2-microglobulin and β-actin cDNA species reveal an expected subcellular distribution pattern of the mRNA species and a non-clustered appearance. Development does not alter the presentation of β-F_1-ATPase mRNA hybrids, although it affects the relative abundance of β-F_1-ATPase mRNA clusters in the cytoplasm of the hepatocyte. These findings illustrate *in vivo* the existence of two different sorting pathways for the nuclear-encoded mRNA species of mitochondrial proteins. High-resolution immunocytochemistry and immunoprecipitation experiments allowed the identification of the β-subunit precursor in the cytoplasm of the hepatocyte, also suggesting a post-translational import pathway for this precursor protein. It is suggested that the localization of β-F_1-ATPase mRNA in a subcellular structure of the hepatocyte might have implications for the control of gene expression at post-transcriptional levels during mitochondrial biogenesis in mammals.

INTRODUCTION

Mitochondrial biogenesis results from the co-ordinated expression of the two cellular genomes in which molecular components of the organelle are encoded [1]. In mammalian cells, the regulation of the expression of nuclear-encoded mitochondrial proteins involved in the bioenergetic function of the organelle has been described mostly at the transcriptional level [2–6]. However, recent findings have provided evidence for the existence of additional mechanisms operating at the post-transcriptional level [7–10]. In rat liver, the onset of mitochondrial biogenesis immediately after birth illustrates a set of mechanisms in which the expression of the nuclear-encoded gene for the β-subunit of the mitochondrial H^+-ATP synthase (β-F_1-ATPase) is exerted at the levels of the stability [10] and translational efficiency [9,10] of the transcript. Interestingly, the expression of the mitochondrial genome at this stage of mammalian development is also exerted at the same two post-transcriptional levels of gene expression [11,12].

It is nowadays recognized that the subcellular localization of certain mRNA species influences the spatial distribution of proteins and affects the differentiation and function of eukaryotic cells [13–20]. The accumulation of a 'masked' [21] β-F_1-ATPase mRNA in the fetal liver [9] seems to respond to a predetermined differentiation programme of the organism, that is, the rapid postnatal differentiation of mitochondria [22]. Immediately after birth, the translational efficiency of the accumulated β-F_1-ATPase mRNA experiences a profound increase [9] that results in a significant increase in the relative amount and activity of this protein in mitochondria, as assessed both in the isolated organelle [4,10,22] and in the liver *in situ* [10]. Therefore we were interested in studying the subcellular localization of β-F_1-ATPase mRNA during liver development as part of an effort aimed at understanding the post-transcriptional mechanisms that regulate the biogenesis of mammalian mitochondria.

MATERIALS AND METHODS

Animals

Timed-pregnant albino Wistar rats weighing 200 g were fed with standard laboratory chow and water *ad libitum*. Pregnancy was confirmed on day 19 of gestation. The fetuses (0 h old) (5.2 ± 0.1 g) were delivered by rapid hysterectomy from cervically dislocated pregnant rats on day 22 of gestation. The newborns were maintained without feeding as previously described [22] and killed by decapitation at 1 h postnatal (1 h old). Adult male rats (approx. 250 g) were also used.

Tissue processing for electron microscopy (EM)

Processing of samples for EM was performed as recently reported in detail [23]. Briefly, small pieces of livers from 0 h, 1 h and adult rats were fixed by immersion in freshly prepared 4% (w/v) paraformaldehyde (Merck, Darmstadt, Germany) in 0.1 M Sörensen phosphate buffer, pH 7.2, for 2 h at 4 °C. Tissue samples were rinsed in buffer and the free aldehyde groups were quenched by immersion in 50 mM NH_4Cl in PBS [0.01 M phosphate buffer/0.15 M NaCl (pH 7.2)] for 60 min at room temperature (two changes of 30 min each), rinsed in PBS and finally processed for embedding in Lowicryl K4M (Chemische Wercke Lowi, Waldkraiburg, Germany) in accordance with manufacturer's instructions. Gold interference colour ultrathin sections were collected in Formvar/carbon-coated nickel grids and stored until use. Observation was performed in a JEOL 1010 and JEOL 1200 ex electron microscope at 80 kV accelerating voltage.

Abbreviations used: EM, electron microscopy; α- and β-F_1-ATPase, subunits α and β of the mitochondrial H^+-ATP synthase; RNP, ribonucleoprotein.

* Permanent address: Departamento de Biología Celular y Anatomia Patológica, Facultad de Medicina, Universidad de Barcelona, Casanova 143, 08036 Barcelona, Spain.

† Permanent address: Centro Nacional de Biotecnología, Consejo Superior de Investigaciones Científicas, Cantoblanco, 28049 Madrid, Spain.

‡ To whom correspondence should be addressed.

Digoxigenin-labelled cDNA probes

The cDNA probes used in this study were: rat liver β-F_1-ATPase [24] and α-F_1-ATPase [25], rat liver β_2-microglobulin and human β actin. The cDNA probes were labelled with digoxigenin as follows: 300 ng of the cDNA and 8 μl of pd$(N)_6$ random primer (Boehringer Mannheim, Germany) were mixed (15 μl final volume). Probes were boiled for 5 min and quickly chilled. Then 2 μl of 10 × Vogel buffer [0.5 M Pipes (pH 6.6)/50 mM $MgCl_2$/100 mM 2-mercaptoethanol], 2 μl of nucleotide mix with digoxigenin-labelled dUTP (Boehringer Mannheim) and 1 μl of Klenow enzyme were added and the mixture was incubated at 14 °C overnight. The labelling reaction was stopped by the addition of 50 mM EDTA and heating at 65 °C for 10 min. cDNA probes were also labelled by nick-translation. For this purpose, 100 ng of the cDNA insert were incubated in 10 × NTB (nick-translation buffer) [0.5 M Tris/HCl (pH 7.5)/0.1 M $MgCl_2$/1 mM dithiothreitol/0.5 mg/ml BSA] containing the nucleotide mix with digoxigenin-labelled dUTP, DNase I (0.1 μg/ml) and DNA polymerase I (5 units/μl) for 60 min at 15 °C. The reaction was stopped by the addition of 10 mM Tris/HCl (pH 8)/1 mM EDTA. The labelled probes were purified by gel filtration. The probes were precipitated and stored at −70 °C. Labelled probes were resuspended in 10–50 μl of 10 mM Tris/HCl (pH 8)/1 mM EDTA and the amount of digoxigenin incorporated into cDNA was determined by luminescence by following the instructions of the Dig luminescence detection kit (Boehringer Mannheim).

Subcellular localization of mRNA species by EM hybridization *in situ*

Nickel grids bearing sections were floated on small drops (5 μl) of the hybridization solution [26]. This solution contained 50 % deionized formamide, 10 % dextran sulphate, 2 × SSC (1 × SSC is 0.15 M NaCl/0.015 M sodium citrate), 400 μg/ml salmon sperm DNA and any of the labelled probes used in this study: (1) 2.5–16 μg/ml digoxigenin-labelled β-F_1-ATPase cDNA; (2) 2.5–5 μg/ml digoxigenin-labelled α-F_1-ATPase cDNA; (3) 2.5–5 μg/ml digoxigenin-labelled β-actin cDNA; (4) 1–2 μg/ml digoxigenin-labelled β_2-microglobulin cDNA. Hybridization was performed overnight at different temperatures (45, 50 and 55 °C) in a hybridization oven. After hybridization, grids were extensively jet-washed with PBS at room temperature. Immunocytochemical detection of digoxigenin was performed as follows: grids were placed on a small droplet of mouse anti-digoxigenin monoclonal antibody (2–5 μg/ml in PBS) (Boehringer Mannheim), for 60 min at room temperature. After brief rinses in PBS, grids were incubated for 45 min with 50 μg/ml rabbit anti-(mouse IgG + IgM) (Dako A/S, Glostrup, Denmark) in PBS containing 0.1 % Tween-20 at room temperature. Grids were then incubated with Protein A complexed with gold particles (BioCell Research Laboratories, Cardiff, South Glam., U.K.) of diameter 10 or 15 nm, which were diluted to D_{525} values of 0.08 and 0.4 respectively in PBS containing 1 % (w/v) BSA, 0.1 % Triton X-100 and 0.1 % Tween-20. After 45 min of incubation with the Protein A–gold, grids were washed twice in PBS and distilled water, and dried in air. Counterstaining was performed with 2 % (w/v) aqueous uranyl acetate (6 min) and 1 % (w/v) lead citrate (45 s).

An alternative method for the detection of the digoxigenin-labelled β-F_1-ATPase cDNA probe was also used. With this procedure, after hybridization and extensive washing, grids were blocked with a solution containing 0.5 % skimmed milk in PBS. After, the grids were incubated with sheep anti-digoxigenin polyclonal antibody (50 μg/ml in 0.5 % skimmed milk/PBS) (Boehringer Mannheim) for 60 min at room temperature. After brief rinses in PBS, grids were incubated for 45 min with donkey anti-(sheep immunoglobulins) complexed with 10 nm gold particles (BioCell Research Laboratories) diluted to a D_{525} of 0.13, in PBS containing 1 % (w/v) BSA, 0.1 % Triton X-100 and 0.1 % Tween-20. The grids were then processed as above.

Several series of controls were conducted in parallel to assess the specificity of the hybridization signals: (1) pretreatment of ultrathin sections with 50 μg/ml pancreatic bovine RNase (Boehringer Mannheim) in 0.4 M NaCl/10 mM Tris/HCl (pH 7.5)/5 mM EDTA for 90 min at 37 °C, (2) competition experiments with a 50-fold excess of unlabelled cDNA species, followed by incubation with the digoxigenin-labelled cDNA probe, (3) hybridization procedure without the digoxigenin-labelled cDNA probe, (4) hybridization procedure with unlabelled cDNA probe, and (5) standard controls for the immunocytochemical detection of digoxigenin.

Production of β-F_1-ATPase antibodies

Purification and generation of antibodies against the β-subunit of the mitochondrial F_1-ATPase complex was performed as previously described in detail for the whole F_1-ATPase complex with slight modifications [22]. Briefly, adult rat liver mitochondria were prepared on sucrose gradients [27]. The F_1-ATPase complex was extracted with chloroform from purified inner mitochondrial membrane vesicles [22]. The purified F_1-ATPase complex was fractionated by SDS/PAGE [7.5 % (w/v) gel] in the presence of 4 M urea. After staining, the β-subunit band was cut from the gels. The pieces of the gels containing the β-subunit of the F_1-ATPase complex were freeze-dried and ground in a mortar with liquid nitrogen, then further resuspended in water. For antibody production, 1 vol. of the resuspended β-subunit was emulsifed (1:1) with complete Freund adjuvant and administered intradermally in multiple sites of the back of New Zealand rabbits. Four boosting doses of protein emulsified (1:1) with incomplete Freund adjuvant were administered subcutaneously (one) and intradermally (three) every 2 weeks. The titre of the anti-β-F_1-ATPase serum was checked by Western blotting procedures against mitochondrial and homogenate fractions from rat liver as previously described in detail [4,9,10].

Immunocytochemical localization of β-F_1-ATPase protein in rat hepatocytes

The subcellular distribution of β-F_1-ATPase immunoreactive material was studied in ultrathin sections of rat liver. Briefly, grids were transferred to droplets of anti-β-F_1-ATPase serum (diluted 1:2) for 60 min at room temperature. Afterwards, grids were incubated with 50 μg/ml of biotinylated goat anti-(rabbit IgGs) (Dakopatts, Glostrup, Denmark), to amplify the immunoreactive signal of the β-F_1-ATPase antibody [28]. Biotinylated antibodies were revealed by incubation with goat anti-biotin complexed with 10 nm gold particles (BioCell Research Laboratories) diluted to a D_{525} of 0.13 in PBS containing 1 % (w/v) BSA, 0.1 % Triton X-100 and 0.1 % Tween-20. Several series of standard controls for immunocytochemical techniques were conducted in parallel to assess the specificity of the immunoreactive signals.

Labelling *in vivo* and immunoprecipitation of the cytosolic β-subunit precursor of the F_1-ATPase complex

Newborns (1 h old) were intraperitoneally injected with 250 μCi of L-[^{35}S]methionine (1 kCi/mmol) to label *in vivo* the β-F_1-

ATPase precursor protein; 10 min after receiving the tracer, newborns were killed by decapitation and their livers (approx. 0.3 g) were homogenized and mitochondria were isolated [22]. Post-mitochondrial supernatants were divided into two equal volume aliquots (approx. 400 μl). One aliquot was centrifuged at 105000 ***g*** for 60 min at 4 °C. The resulting post-ribosomal supernatant and previous post-mitochondrial supernatants were used for immunoprecipitation experiments. To measure the rate of [^{35}S]methionine incorporated into protein, 2 μl aliquots of liver fractions were precipitated with trichloroacetic acid. The precipitates were washed and counted [22].

The F_1-ATPase β-subunit precursor was immunoprecipated from post-mitochondrial and post-ribosomal supernatants with 5 μl of rabbit anti-(rat liver mitochondrial F_1-ATPase) serum [22] essentially as described [4]. Briefly, the antigen–antibody reaction was performed for 1 h at 37 °C and overnight at 4 °C in a final volume of 0.8 ml, containing 400 μl of sample plus 400 μl of 2 % (w/v) Triton X-100 and 300 mM NaCl. The F_1-ATPase antibody complexes were collected by centrifugation at 12000 ***g*** for 15 min at 4 °C with Protein A–Sepharose. The immunoprecipitates were washed three times: (1) 2 % (w/v) Triton X-100/300 mM NaCl, (2) 0.5 M NaCl/0.1 % Triton X-100/10 mM Tris/HCl (pH 8) and (3) 0.05 % Triton X-100/10 mM Tris/HCl (pH 8). The washed precipitates were dissociated in loading buffer and processed by SDS/PAGE [12.5 % (w/v) gel] as described previously [4,9]. Gels were further processed for fluorography and exposed to X-ray films.

Quantification of labelling signals

Quantification of gold particles for the signals revealing transcript (α- and β-F_1-ATPase mRNA species) hybridization (free or in clusters) was performed by two independent investigators directly at the EM screen in a double-blind fashion with a code that was only broken when the quantification was finished. The results were expressed as the number of gold particles per unit of cellular area. The unit of cellular area was defined as the area of cytoplasm or nucleus equivalent to approx. 25 μm^2 (the micrograph size area taken at a magnification of $\times$8000). The range of the number of different fields taken at random (16–32) or clusters (40–200) examined is given in parenthesis.

Other methods

Extraction of total liver RNA from freeze-clamped rat livers, separation of RNA species by electrophoresis in agarose gels, transfer of denatured RNA species to GeneScreen® membranes and hybridization procedures with [^{32}P]dCTP-labelled cDNA probes have been previously described in detail [9,10].

Fractionation of proteins by SDS/PAGE, electrophoretic transfer of the proteins to poly(vinylidene difluoride) membranes, Western blotting and detection of the immunoreactive β-F_1-ATPase protein with a goat anti-(rabbit IgG)-peroxidase conjugate (Pierce, Rockford, IL, U.S.A.), were performed as described [9,10].

RESULTS

β-F_1-ATPase mRNA appears in clusters in the cytoplasm of rat hepatocytes

The appearance of hybridization signals for the nuclear-encoded β-F_1-ATPase mRNA in rat hepatocytes is shown in Figure 1. Most gold particles revealing β-F_1-ATPase mRNA formed clusters of hybridization signals (Figure 1A, and inset; see also Table 1). A few gold particles were also found scattered throughout the cytoplasm of the cell (Table 1); however, experiments with the unlabelled probe revealed that a significant fraction of the scattered hybridization signal is due to the background of the technique (Table 1). These findings indicate that clusters of β-F_1-ATPase mRNA hybridization represent the specific presentation of β-F_1-ATPase mRNA in rat liver. It should be noted that the pattern of β-F_1-ATPase mRNA hybridization in liver was the same irrespective of the method used for labelling the cDNA probe. Besides, a different immunological procedure to detect the digoxigenin-labelled probe also confirmed the clustered appearance of the oxidative phosphorylation transcript in the cytoplasm of rat hepatocytes (results not shown). Furthermore pretreatment of ultrathin sections with RNase A and competition experiments with a 50-fold excess of unlabelled cDNA probe showed an almost complete decrease in the clusters of hybridization signals revealing β-F_1-ATPase mRNA (Table 1). Overall, these results illustrate the specificity of the *in situ* hybridization protocol and further provide strong support for the finding that β-F_1-ATPase mRNA is a localized transcript in the liver. In fact, β-F_1-ATPase mRNA hybridization clusters were associated with a non-membrane electron-dense structure of average 0.15 μm in diameter (see Figure 1A, inset).

In the nucleus, gold particles revealing β-F_1-ATPase mRNA were found both scattered (approx. 25 %) (Figure 1B, arrowheads) and forming rounded hybridization clusters (approx. 75 %) (Figure 1C, arrow, and Table 1). It is possible that in the nuclei scattered hybridization signals could represent specific recognition of β-F_1-ATPase mRNA (Table 1). In such a situation, the different presentations of nuclear labelling for β-F_1-ATPase mRNA could indicate the identification of the transcript at different stages of its nuclear processing. Interestingly, some clusters of β-F_1-ATPase mRNA were revealed in close contact with nuclear pores (Figure 1B, open arrow).

In the cytoplasm, clusters of hybridization signals were most frequently found in the proximity of mitochondria or even in close contact with mitochondria (approx. 21 %) (Figure 1A). We suggest that these varied distributions of β-F_1-ATPase mRNA clusters within the cell reflect the 'time-frozen' picture of the dynamic process of mRNA sorting, i.e. in the nucleus, at the site of synthesis of the ribonucleoprotein (RNP) particle; in the proximity of nuclear pores, before or after being exported from the nucleus; in the cytoplasm, free or attached to the mitochondria, RNP particles in transit or at the site of delivery of the encoded precursor. However, it should be stressed that single or linearly arranged gold particles revealing β-F_1-ATPase mRNA were hardly ever found decorating the outer mitochondrial membrane.

Hybridization *in situ* reveals differences in the hepatocyte content of β-F_1-ATPase mRNA clusters during development

The relative cellular content of β-F_1-ATPase mRNA is much higher at early stages of liver development (fetal and early neonatal) than in the adult stage [9,10]. Furthermore the accumulated β-F_1-ATPase mRNA experiences rapid and profound changes in its sedimentation [9] and translational [9,10] behaviours as a result of birth. Therefore we were interested in knowing whether these differences were also manifested at the subcellular level. Figure 2(A) shows the pattern of hybridization of β-F_1-ATPase mRNA in the liver of adult rats [see Figure 1(A) for a comparison with that of the fetal rat liver]. Development did not alter the presentation of β-F_1-ATPase mRNA hybridization signals in the cytoplasm of the hepatocyte; that is, β-F_1-ATPase mRNA was always found forming clusters of hybridization signals. In addition, the number of gold particles

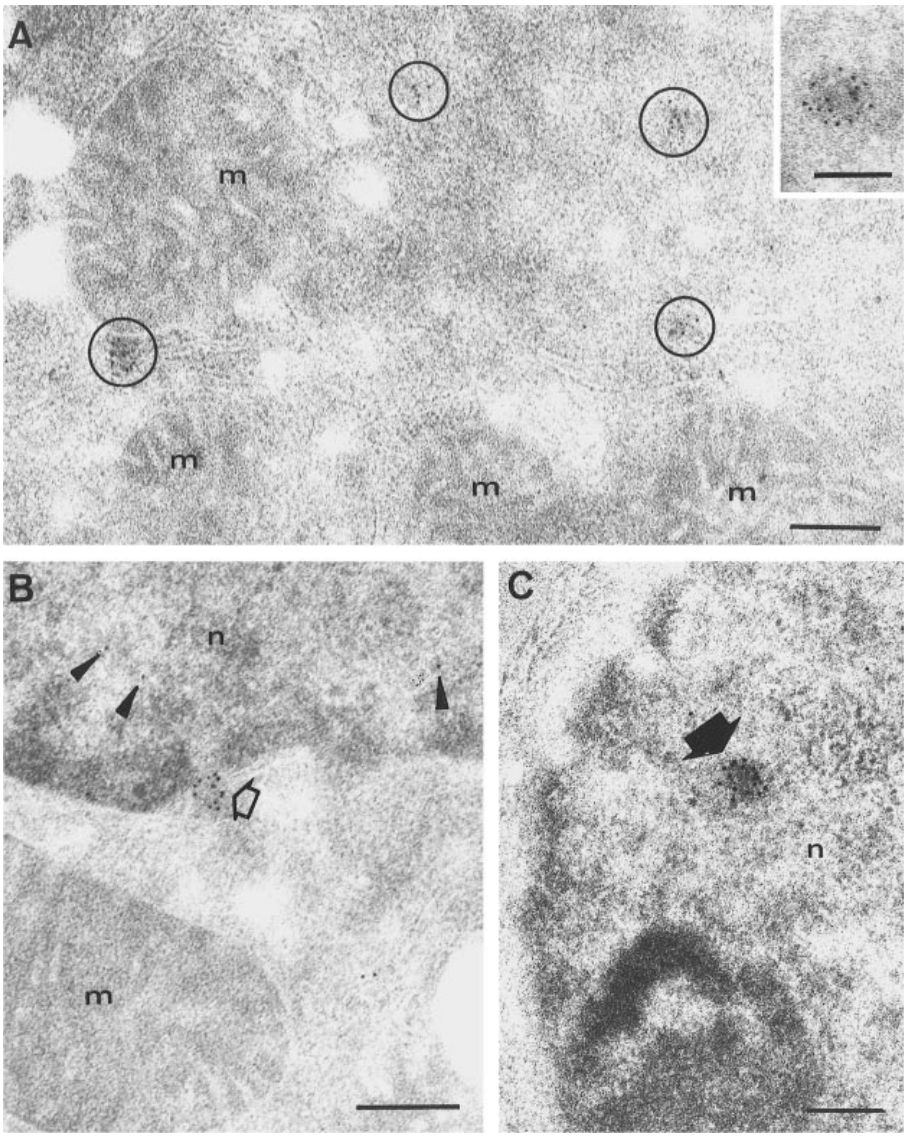

Figure 1 The nuclear-encoded β-F_1-ATPase mRNA presents a clustered appearance in the cytoplasm and nuclei of fetal rat hepatocytes

In the cytoplasm most gold signals revealing β-F_1-ATPase mRNA are revealed forming clusters of hybridization [see inside the circles in (**A**) and the open arrow in (**B**)]. A significant percentage of clusters (approx. 21%) is associated with the outer mitochondrial membrane (**A**). β-F_1-ATPase mRNA clusters are associated with an electron-dense structure of average 150 nm in diameter [see inset in (**A**)]. Gold signals in nuclei are revealed both in a rounded cluster appearance [arrow in (**C**)] and free and scattered in nucleoplasm [arrowheads in (**B**)]. However, a major proportion of hybridization signals are located in nuclear clusters (see Table 1). Moreover, clusters are also found in close association with the nuclear pores [open arrow in (**B**)]. For quantification of hybridization signals and controls see Table 1 and the text. Abbreviations: m, mitochondria; n, nucleus. Bars, 200 nm (**A** and inset), 500 nm (**B** and **C**).

per cluster was the same at the three stages of liver development studied (approx. 9.3 ± 1.0 particles per cluster, $\pm$S.E.M.). However, the relative abundance of cytoplasmic clusters of β-F_1-ATPase mRNA did reveal a significant difference ($P < 0.0005$) between the stages of development considered. β-F_1-ATPase mRNA clusters were approx. 4-fold more abundant in the fetal and neonatal than in the adult hepatocyte (3.9 ± 0.7, 4.6 ± 0.7 and 1.0 ± 0.1 β-F_1-ATPase mRNA clusters per unit of cytoplasm for fetal, 1 h-old neonatal and adults respectively). This finding is in agreement with the differences in the cellular content of β-F_1-ATPase mRNA determined by Northern procedures (Figure 2B) [9,10], further providing strong support that (1) the *in situ* hybridization protocol is specifically recognizing the β-F_1-ATPase mRNA of the rat liver and (2) the specific localization of the mRNA is maintained throughout liver development.

α-F_1-ATPase mRNA is scattered and evenly distributed in the cytoplasm of rat hepatocytes

To verify whether the subcellular appearance of β-F_1-ATPase mRNA follows a common pattern for nuclear transcripts encoding mitochondrial proteins, parallel hybridization experiments were performed *in situ* with a cDNA probe encoding the rat liver α-subunit of the F_1-ATPase complex. In addition, the subcellular distribution of β_2-microglobulin and β-actin, two non-mitochondrial transcripts, were studied. To our surprise, the subcellular appearance of α-F_1-ATPase mRNA hybrids was different from that observed for β-F_1-ATPase mRNA hybrids [compare Figure 3(A) with Figures 1(A) and 2(A)]. Gold particles revealing α-F_1-ATPase mRNA were free and scattered in the cytoplasm of the hepatocyte (80 ± 5 gold particles per unit of

Table 1 Quantification and assessment of the specificity of β-F1-ATPase mRNA hybridization signals in rat hepatocytes

Ultrathin sections were incubated with unlabelled β-cDNA (−digoxigenin) or labelled β-cDNA (+digoxigenin). The numbers of free and clustered gold particles per unit of cytoplasm or nuclear area were measured. The unit of cellular area was defined as the area of cytoplasm or nucleus equivalent to approx. 25 μm^2 (the micrograph size area taken at a magnification of ×8000). The results shown are means ± S.E.M.; the *n* values (number of observations on samples prepared from three different liver preparations) are indicated in parenthesis. †$P < 0.0005$, −digoxigenin compared with +digoxigenin; * $P < 0.0005$, free compared with clustered signals, by Student's *t*-test. Also, the quantification of the number of β-mRNA clusters per unit of cytoplasm or nuclear area in ultrathin sections preincubated with pancreatic bovine ribonuclease (RNase A) or with a 50-fold excess of unlabeled β-cDNA (competed) is shown. For comparative purposes, the number of clusters per unit of cytoplasm or nuclear area in untreated grids processed in parallel is shown. The results are means ± S.E.M.; the *n* values are indicated in parenthesis. ‡$P < 0.01$; ‡‡$P < 0.0005$ compared with untreated by Student's *t*-test.

	β-mRNA signals per unit of cytoplasm			β-mRNA signals per unit of nucleus		
β-cDNA probe	Free	In clusters		Free	In clusters	
−Digoxigenin	9 ± 2 (11)	None		5 ± 1 (11)	None	
+Digoxigenin	22 ± 2 (10)†	156 ± 24 (10)*		16 ± 2 (10)†	60 ± 10 (10)*	
	β-mRNA clusters per unit of cytoplasm			β-mRNA clusters per unit of nucleus		
	Untreated	RNase A	Competed	Untreated	RNase A	Competed
+Digoxigenin	4.5 ± 0.7 (10)	0.9 ± 0.2 (10)‡‡	None	1.2 ± 0.3 (10)	0.2 ± 0.1 (9)‡	None

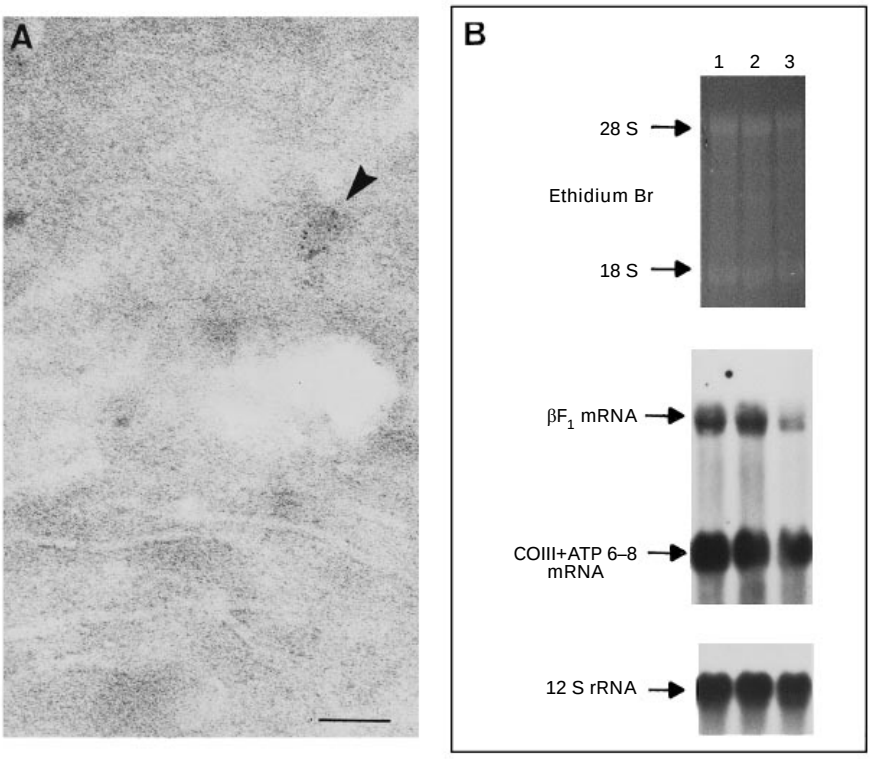

Figure 2 Development does not alter the presentation of β-F_1-ATPase mRNA in rat liver

Gold signals revealing β-F_1-ATPase mRNA in the cytoplasm of adult rat hepatocytes are revealed forming hybridization clusters [arrowhead in (**A**)]. However, the number of hybridization clusters per unit of cytoplasm area (approx. 25 μm^2) is lower in adult than in fetal or in 1 h-old neonatal hepatocytes (**A**) (see text). The lower relative abundance of β-F_1-ATPase mRNA clusters in the adult hepatocyte mimics the results obtained by Northern procedures (**B**). Total RNA (30 μg) extracted from fetal (lane 1), 1 h-old neonatal (lane 2) and adult (lane 3) livers was analysed by Northern blot hybridization procedures with the indicated probes. A parallel ethidium bromide-stained gel shows 28 S and 18 S rRNA species. COIII refers to subunit III of cytochrome *c* oxidase; ATP 6–8, subunits 6 and 8 of H^+–ATP synthase. Bar in (**A**), 200 nm.

cytoplasm) (Figure 3A, arrowheads). Some preferential clustering of hybridization signals could be occasionally observed, although this arrangement of α-F_1-ATPase mRNA hybridization signals represented a small percentage of the total (approx. 5%) (5 ± 1 gold particles per unit of cytoplasm) and were never associated with a rounded electron-dense cytoplasmic structure (Figure 3A). Likewise, as described for β-F_1-ATPase mRNA signals, single gold particles were seldom located on the outer mitochondrial membrane.

Hybridization experiments with β_2-microglobulin cDNA (Fig-

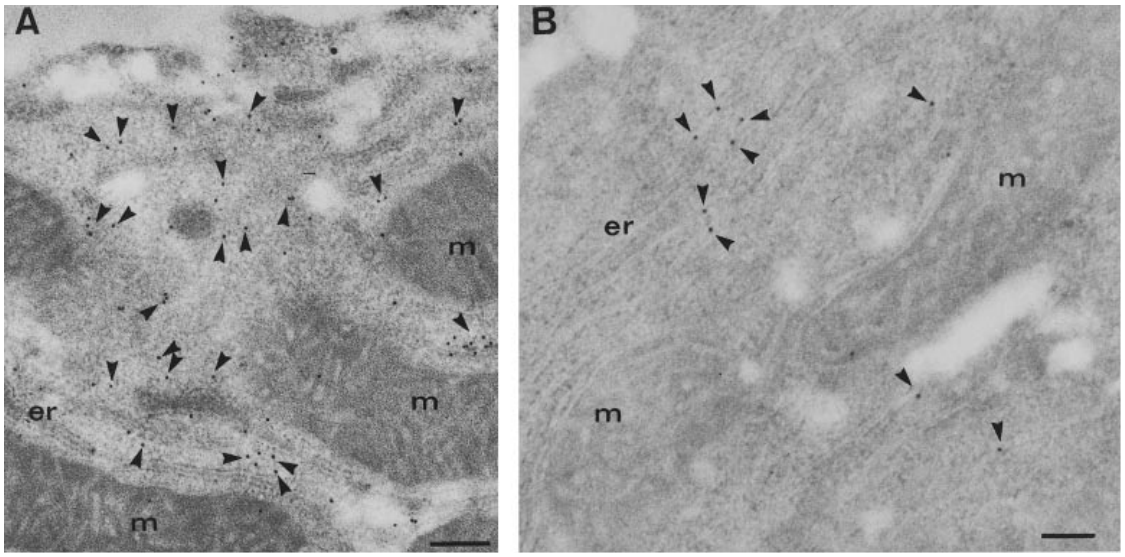

Figure 3 Non-clustered appearance of the α-F_1-ATPase mRNA in rat liver

Fetal rat liver ultrathin sections were processed in parallel for detection *in situ* of α-F_1-ATPase (**A**) and β_2-microglobulin (**B**) mRNA species. Note that for α-F_1-ATPase mRNA, gold particles are free and scattered in the cytoplasm [arrowheads in (**A**)]. Occasionally, clustered gold particles were also revealed but not associated with an electron-dense subcellular structure. Hybridization *in situ* revealing β_2-microglobulin mRNA (**B**) exhibited the expected association of gold particles with the endoplasmic reticulum membrane (arrowheads). The quantification of the number of free and clustered gold particles of α-mRNA per unit of cytoplasm area is indicated in the text. Abbreviations: m, mitochondria; er, endoplasmic reticulum. Bars, 200 nm.

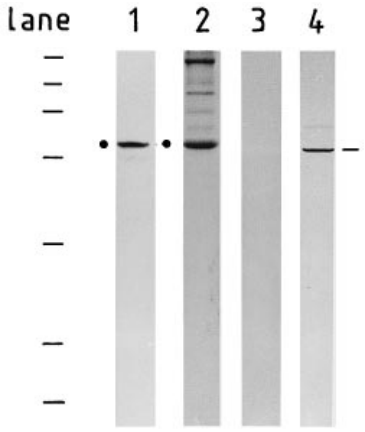

Figure 4 The newly synthesized β-subunit precursor is present in the post-mitochondrial fraction of rat liver cytosols

Newborn rats were injected intraperitoneally with [^{35}S]methionine to label the β-F_1-ATPase precursor *in vivo*. Equal volumes of labelled post-mitochondrial (lane 2) or post-ribosomal (lane 3) supernatants were immunoprecipitated with anti-F_1-ATPase serum. The resulting immunoprecipitates were resolved by SDS/PAGE. The same exposure times of the resulting fluorograms are shown. Lane 1: shows the migration of the radiolabelled β-subunit precursor synthesized *in vitro* in a nuclease-treated rabbit reticulocyte lysate. The lysate was primed with 1 μg of β-F_1-ATPase mRNA synthesized *in vitro* derived from the pJMI-β-F_1 plasmid containing the full-length β-F_1-ATPase cDNA from rat liver (J. M. Izquierdo and J. M. Cuezva, unpublished work; the method can be obtained from the authors on request). The migration of the β-subunit precursor of the F_1-ATPase complex is shown (●). Lane 4 illustrates the migration of the β-subunit of the F_1-ATPase complex in a Western blot of mitochondrial proteins. Note that (1) most (more than 95%) of the immunoprecipitated β-subunit precursor is present in the post-mitochondrial fraction and (2) there is negligible immunoprecipitation of radiolabelled proteins migrating faster than the β-subunit precursor. The positions of 200, 97.4, 69, 46, 30, 21.5 and 14.3 kDa Rainbow coloured protein molecular mass markers (Amersham RPN 756) are shown at the left.

ure 3B) provided a pattern for the subcellular distribution of this transcript, in agreement with the expected distribution of a protein that follows the secretory pathway [29,30]. Gold particles revealing β_2-microglobulin mRNA presented a non-clustered appearance and were predominantly found associated with the rough endoplasmic reticulum cisterna (Figure 3B, arrowheads). Likewise, hybrids revealing β-actin mRNA presented a non-clustered appearance (results not shown).

We should stress that the non-clustered appearance of the hybridization signals revealing α-F_1-ATPase, β_2-microglobulin and β-actin mRNA species further supports the specific cluster arrangement of β-F_1-ATPase mRNA hybridization. Hybridization procedures with the different cDNA probes used in this study were performed in parallel and in consecutive sections of the same tissue blocks. Furthermore, irrespective of the tissue blocks and developmental stages of the liver examined, hybridizations *in situ* always provided the same patterns of presentation of the different mRNA species studied (Figures 1, 2 and 3). Therefore it is very unlikely that fixation and embedding procedures and/or accessibility problems of the probe could induce the clustering of the β-F_1-ATPase mRNA signal but not of the α-F_1-ATPase, β_2-microglobulin and β-actin.

Identification of the β-F_1-ATPase precursor in the cytoplasm of the hepatocyte

Immunoprecipitation of post-mitochondrial supernatants from 1 h-old neonatal liver labelled *in vivo* with anti-F_1-ATPase serum and further SDS/PAGE fractionation of the resulting immunoprecipitates revealed the presence of a major newly synthesized product of average molecular mass approx. 52 kDa (Figure 4, lane 2). The electrophoretic migration of this product coincided with that of the β-F_1-ATPase precursor synthesized *in vitro* obtained from the transcription *in vitro* of a full length β-F_1-ATPase cDNA clone (Figure 4, lane 1) and with that of the immunoprecipitated product from the translation of rat liver RNA *in vitro* (see [9], Figs. 6 and 7). Furthermore the electrophoretic migration of the immunoprecipitated product (Figure 4, lane 2) was slightly less than that of the mature β-F_1-ATPase protein (Figure 4, lane 4), in agreement with previous findings on

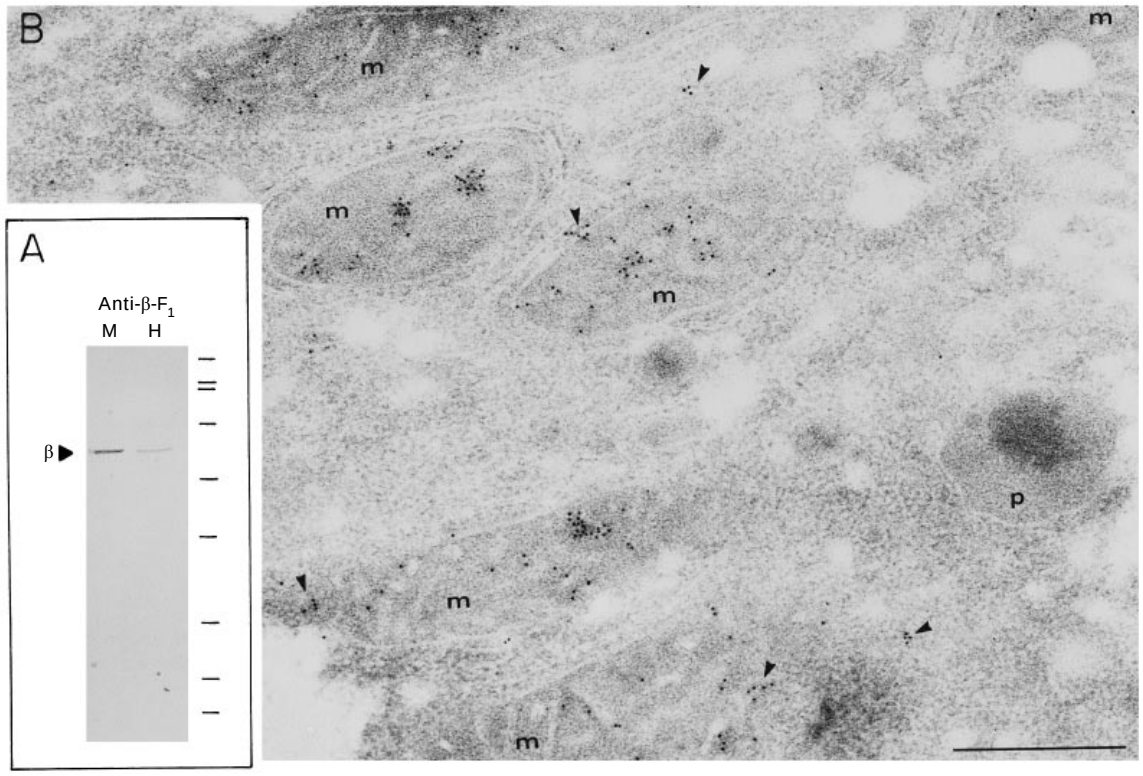

Figure 5 Immunocytochemical procedures reveal the presence of the β-subunit precursor in the cytoplasm of the hepatocyte

(**A**) SDS/PAGE fractionation of 10 μg of mitochondrial (M) and 20 μg of total (H) rat liver proteins Western blotted with a 1:4000 dilution of anti-β-F_1-ATPase serum reveals the specificity of the antibody toward the mitochondrial β-subunit protein. The positions of 200, 116, 97.4, 66.2, 45, 31, 21.5, 14.4 and 6.5 kDa Bio/Rad SDS-PAGE protein standards (broad range) are shown at the right. (**B**) Immunogold labelling (10 nm gold) for β-F_1-ATPase in neonatal rat liver ultrathin sections, with a biotinylated antibody (see the Methods section), decorates mitochondria and the cytoplasm (arrowheads) of the hepatocyte. Omission of the primary antibody does not provide significant labelling of hepatocyte structures. The quantification of the number of gold particles/μm^2 of cytoplasm or mitochondrial section is indicated in the text. Abbreviations: m, mitochondria; p, peroxisome. Bar, 500 nm.

the processing of the β-subunit precursor in rat liver [31]. Therefore it is reasonable to suggest that most of the immunoprecipitated product from post-mitochondrial supernatants represents the precursor protein of the β-subunit of the F_1-ATPase complex. However, immunoprecipitation of post-ribosomal supernatants labelled *in vivo* (Figure 4, lane 3) did not provide significant detection of the β-subunit precursor in this fraction. These findings suggest that the β-precursor is associated with other components of the cytoplasm of the hepatocyte. In addition, the results suggest that *in vivo* a fraction of the β-subunit precursor is imported into mitochondria post-translationally.

To illustrate that the β-precursor could be detected in the cytoplasm of the hepatocyte by an additional approach, a monospecific antibody against the β-subunit of the F_1-ATPase complex from rat liver mitochondria was first developed. This antibody showed an approx. 50 fold higher titre in Western blotting experiments (Figure 5A) than a previously obtained antibody raised against the whole F_1-ATPase complex [22]. The monospecific antibody recognized the β-subunit of the F_1-ATPase complex in liver homogenates and in isolated mitochondria (Figure 5A). However, no clear identification of a band corresponding to the β-subunit precursor could be obtained in Western blots of liver homogenates (Figure 5A) or in post-mitochondrial supernatants (results not shown). This result (Figure 5A) might seem inconsistent with the detection of the radiolabelled precursor in post-mitochondrial supernatants (Figure 4). However, it should be considered that the sensitivity of the detection of the β-subunit precursor by metabolic labelling is much higher than that provided by Western procedures. Anyway, the antibody, with the inclusion of an amplification step of the primary immunoreactive signal [28], was used in high-resolution immunocytochemical procedures. It was suspected that immunocytochemistry could partly overcome the limitations of Western procedures when using samples containing poorly represented proteins, specially in situations where the protein to detect is concentrated (or localized) within certain regions of the cytoplasm, as could be predicted for the β-subunit precursor from the cluster arrangement of β-F_1-ATPase mRNA in rat liver (Figures 1 and 2).

Immunocytochemical procedures with the anti-β-F_1-ATPase serum did reveal the presence of positive immunoreactive signals in the cytoplasm of the hepatocyte (58 ± 6 gold particles/μm^2) (arrowheads in Figure 5B). Other subcellular structures (nucleus, peroxisomes, endoplasmic reticulum membranes, Golgi stacks) than mitochondria (229 ± 9 gold particles/μm^2) (Figure 5B) revealed no significant labelling above the controls of the immunocytochemistry (i.e. omission of the primary antibody: 0.6 ± 0.1 gold particles/μm^2 of section). Both the number of positive β-F_1-ATPase signals in the cytoplasm and their relative subcellular locations [close to or attached to the outer mitochondrial membrane (Figure 5B)] are similar to those detected by

hybridization procedures for β-F_1-ATPase mRNA clusters (compare Figure 5B with Figure 1A). In agreement with the results of immunoprecipitation experiments (Figure 4), it is reasonable to suggest that the specific immunolabelling of the cytoplasm (Figure 5B) illustrates the recognition of the precursor of the β-subunit of the F_1-ATPase complex, thus providing additional support for the finding that *in vivo* a fraction of the precursor is being post-translationally imported into mitochondria.

DISCUSSION

In this study the subcellular localization and presentation of two nuclear-encoded oxidative phosphorylation transcripts (α- and β-F_1-ATPase mRNA species) have been studied in rat hepatocytes. Strikingly, the subcellular presentation of these mRNA species, which encode two subunits of the same inner membrane complex (F_1-ATPase), is different. We show that β-F_1-ATPase mRNA species appear in rounded electron-dense clusters that are sometimes associated with mitochondria. In contrast, the mRNA species for the α-subunit of the ATPase do not show this particular clustering. The study of the localization of β-F_1-ATPase mRNA in liver was extended at specific stages of development that are characterized by profound changes in the availability, stability, translational efficiency and sedimentation behaviour of β-F_1-ATPase mRNA [9,10]. The idea pursued was that the analysis of the compartmentation of this transcript could help to understand post-transcriptional mechanisms controlling the expression of β-F_1-ATPase mRNA during development [9,10] and therefore the biogenesis of mitochondria in mammals.

In spite of a lower transcriptional activity of the β-F_1-ATPase gene [10], fetal and neonatal livers show a higher relative abundance of β-F_1-ATPase mRNA than adult livers (Figure 2B) [9,10]. This accumulation of β-F_1-ATPase mRNA transcript is caused by an increased stability of the template at early stages of development [10]. Hybridization experiments *in situ* confirmed these differences in β-F_1-ATPase mRNA availability (Figure 2) and provided further evidence that the clustered presentation of the transcript is not affected during liver development. These results therefore suggest that changes in the stability and translational efficiency of β-F_1-ATPase mRNA during development cannot be accounted for by the sequestration of the transcript in cluster structures but are instead mediated by regulatory molecules that interact with the structure where β-F_1-ATPase mRNA is located.

The different presentations of α- and β-F_1-ATPase mRNA in the cytoplasm of the hepatocyte suggest the existence of two different mechanisms [32] for subcellular sorting of these nuclear-encoded oxidative phosphorylation transcripts. In other words, the dynamic and putative proteins involved in binding these two mRNA species are different. Several hybridization studies *in situ* have shown that certain mRNA species display a patchy pattern in the cytoplasm [15,33,34], suggesting the association of transcripts to RNP particles. The location of β-F_1-ATPase mRNA in electron-dense structures suggests that this mRNA also forms an RNP particle. The assembly of such structures most probably results from the interaction of a localization element, usually present in the 3′ untranslated region of mRNA species [35], and specific *trans*-acting protein(s) recognizing the element (reviewed in [18,19,36]). It is expected that these mRNA-binding proteins play pivotal roles in the transport, stability and/or translational efficiency of the bound mRNA. Remarkably, a recent report has provided genetic evidence that proteins interacting with mRNA 3′ ends mediate the delivery of proteins into mitochondria [37]. It is therefore suggested that future investigations aimed at characterizing specific β-F_1-ATPase mRNA binding proteins will provide functional explanations for this particular cluster arrangement of the β-F_1-ATPase mRNA.

It seems that β-F_1-ATPase mRNA particles are formed in the nuclei of the hepatocyte (Figure 1) and are further exported to the cytoplasm through the nuclear pore complex (Figure 1) [32]. The study of RNA movement, export and localization is still at an early stage. However, at this point we should stress the recent characterization of a gene (*MTS1*) encoding a putative RNA-binding protein that acts as an extragenic suppressor of a yeast mutant with a targeting defect in the presequence of the β-subunit of ATP synthase [38]. The encoded protein of this gene (also called Nop3p/NpI3p) [39] exhibits considerable structural similarity to hnRNP proteins from other organisms [40,41] and, like A1 hnRNP, shuttles between the nucleus and the cytoplasm [39]. Therefore it seems reasonable to suggest that the mammalian homologue of the Mts1 protein [38] might be involved in nucleocytoplasmic transport of the β-F_1-ATPase mRNA transcript.

Import studies with isolated yeast mitochondria have allowed the classification of mitochondrial precursor into two groups depending on whether they require (group 2) or do not require (group 1) extramitochondrial ATP [42,43]. These findings have led to the proposed existence of two different cytoplasmic states for mitochondrial precursor proteins [42,43]. The results reported in this study regarding the different presentation of α- and β-F_1-ATPase mRNA in the cytoplasm of the hepatocyte might provide support, at the subcellular level, for the above suggestion. The question now is: What might be the biological significance of such dissimilar sorting mechanisms for two mRNA species encoding subunits of the same mitochondrial complex? It seems reasonable to suggest that the existence of these two mechanisms might ensure that the two precursor proteins do not interact in the cytoplasm of the cell, which might hamper their import into mitochondria.

It has been widely accepted that mitochondrial precursors undergo post-translational import into mitochondria both *in vivo* and *in vitro* [44–46]. However, recent suggestions claim a co-translational import mechanism for sorting of these proteins *in vivo*, at least during active periods of mitochondrial biogenesis [47]. The existence of co-translational import for sorting mitochondrial proteins would imply, by analogy with the location shown for β_2-microglobulin mRNA (see Figure 3B), the localization of mitochondrial mRNA species on the outer mitochondrial membrane. However, hybridization experiments for α- and β-F_1-ATPase mRNA species reveal negligible, if any, gold decoration of the outer mitochondrial membrane, albeit for β-F_1-ATPase mRNA clusters. Furthermore immunoprecipitation (Figure 4) and immunoelectron microscopy (Figure 5) experiments illustrated the existence of the β-F_1-ATPase precursor in the cytoplasm of the hepatocyte. In other words, our findings suggest that the synthesized β-precursor is post-translationally imported into mitochondria, and that *in vivo* co-translational import processes for these two proteins (α- and β-F_1-ATPase subunits) in mammalian cells could be estimated as negligible, even during active periods of mitochondrial biogenesis. Anyway, although our findings do not provide evidence supporting co-translational import processes, a significant percentage (21 %) of β-F_1-ATPase mRNA clusters (Figure 1A) or of the cytoplasmic β-precursor (Figure 5) is found attached to the outer mitochondrial membrane. These findings suggest that perhaps *in vivo* and under the dynamic state of cellular mRNA movement there is a requirement for certain localized mRNA

species, such as clusters of β-F_1-ATPase mRNA, and the mitochondria. We propose that the functional implication of this association in the control of mitochondrial biogenesis deserves to be explored in the future.

We thank Professor J. Satrústegui for a critical reading of the manuscript; Dr. P. L. Pedersen, J. Ortin and M. Lorenzo for the supply of α- and β-F_1-ATPase cDNA species, β-actin cDNA and β_2-microglobulin cDNA probes respectively; and M. Chamorro and D. Jelenic for technical and secretarial assistance respectively. G. E. thanks the University of Barcelona for supporting his stay at Centro de Biología Molecular 'Severo Ochoa'. J. R. is a recipient of a predoctoral fellowship from Ministerio de Educación y Ciencia. The work was supported by grants (PB91-0032 and PB94-0159) from Dirección General de Investigación Científica y Técnica and by grant AE00238/95 from Comunidad de Madrid, Spain. We acknowledge an institutional grant from Fundación Ramón Areces, Spain.

REFERENCES

1 Attardi, G. and Schatz, G. (1988) Annu. Rev. Cell Biol. **4**, 289–333
2 Scarpulla, R. C., Kilar, M. C. and Scarpulla, K. M. (1986) J. Biol. Chem. **261**, 4660–4662
3 Williams, R. S., Garcia Moll, M., Mellor, J., Salmons, S. and Harlan, W. (1987) J. Biol. Chem. **262**, 2764–2767
4 Izquierdo, J. M., Luis, A. M. and Cuezva, J. M. (1990) J. Biol. Chem. **265**, 9090–9097
5 Torroni, A., Stepien, G., Hodge, J. A. and Wallace, D. C. (1990) J. Biol. Chem. **265**, 20589–20593
6 Izquierdo, J. M. and Cuezva, J. M. (1993) FEBS Lett. **323**, 109–112
7 Polosa, P. L. and Attardi, G. (1991) J. Biol. Chem. **266**, 10011–10017
8 Izquierdo, J. M. and Cuezva, J. M. (1993) Biochem. Biophys. Res. Commun. **196**, 55–60
9 Luis, A. M., Izquierdo, J. M., Ostronoff, L. K., Salinas, M., Santaren, J. F. and Cuezva, J. M. (1993) J. Biol. Chem. **268**, 1868–1875
10 Izquierdo, J. M., Ricart, J., Ostronoff, L. K., Egea, G. and Cuezva, J. M. (1995) J. Biol. Chem. **270**, 10342–10350
11 Ostronoff, L. K., Izquierdo, J. M. and Cuezva, J. M. (1995) Biochem. Biophys. Res. Commun. **217**, 1094–1098
12 Ostronoff, L. K., Izquierdo, J. M., Enríquez, J. A., Montoya, J. and Cuezva, J. M. (1996) Biochem. J. **316**, 183–191
13 Lawrence, J. B. and Singer, R. H. (1986) Cell **45**, 407–415
14 Garner, C. C., Tucker, R. P. and Matus, A. (1988) Nature **336**, 674–677
15 Ainger, K., Avossa, D., Morgan, F., Hill, S. J., Barry, C., Barbarese, E. and Carson, J. H. (1993) J. Cell Biol. **123**, 431–441
16 Litman, P., Barg, J., Rindzoonski, L. and Ginzburg, I. (1993) Neuron **10**, 627–638
17 Hill, M. A. and Gunning, P. (1993) J. Cell Biol. **122**, 825–832
18 Wilhelm, J. E. and Vale, R. D. (1993) J. Cell Biol. **123**, 269–274
19 Johnston, D. S. (1995) Cell **81**, 161–170
20 Curtis, D., Lehmann, R. and Zamore, P. D. (1995) Cell **81**, 171–178
21 Jackson, R. J. and Standart, N. (1990) Cell **62**, 15–24
22 Valcarce, C., Navarrete, R. M., Encabo, P., Loeches, E., Satrustegui, J. and Cuezva, J. M. (1988) J. Biol. Chem. **263**, 7767–7775
23 San Martín, C., Flores, A. I. and Cuezva, J. M. (1995) J. Cell. Biochem. **59**, 235–245
24 Garboczi, D. N., Fox, A. H., Gerring, S. L. and Pedersen, P. L. (1988) Biochemistry **27**, 553–560
25 Lee, J. H., Garboczi, D. N., Thomas, P. J. and Pedersen, P. L. (1990) J. Biol. Chem. **265**, 4664–4669
26 Puvion-Dutilleul, F., Mazan, S., Nicoloso, M., Christensen, M. E. and Bachellerie, J. P. (1991) Eur. J. Cell Biol. **56**, 178–186
27 Cuezva, J. M., Santaren, J. F., Gonzalez, P., Valcarce, C., Luis, A. M. and Izquierdo, J. M. (1990) FEBS Lett. **270**, 71–75
28 Egger, D., Troxler, M. and Bienz, K. (1994) J. Histochem. Cytochem. **42**, 815–822
29 Pfeffer, S. R. and Rothman, J. E. (1987) Annu. Rev. Biochem. **56**, 829–852
30 Okita, T. W., Li, X. and Roberts, M. W. (1994) Trends Cell Biol. **4**, 91–96
31 Santaren, J. F., Alconada, A. and Cuezva, J. M. (1993) J. Biochem. (Tokyo) **113**, 129–131
32 Izaurralde, E. and Mattaj, I. W. (1995) Cell **81**, 153–159
33 Taneja, K. L., Lifshitz, L. M., Fay, F. S. and Singer, R. H. (1992) J. Cell Biol. **119**, 1245–1260
34 Cripe, L., Morris, E. and Fulton, A. B. (1993) Proc. Natl. Acad. Sci. U.S.A. **90**, 2724–2728
35 Decker, C. J. and Parker, R. (1995) Curr. Opin. Cell Biol. **7**, 386–392
36 McCarthy, J. E. G. and Kollmus, H. (1995) Trends Biochem. Sci. **20**, 191–197
37 Zoladek, T., Vaduva, G., Hunter, L. A., Boguta, M., Go, B. D., Martin, N. C. and Hopper, A. K. (1995) Mol. Cell. Biol. **15**, 6884–6894
38 Ellis, E. M. and Reid, G. A. (1993) Gene **132**, 175–183
39 Flach, J., Bossie, M., Vogel, J., Corbett, A., Jinks, T., Willins, D. A. and Silver, P. (1994) Mol. Cell. Biol. **14**, 8399–8407
40 Piñol-Roma, S. and Dreyfuss, G. (1991) Science **253**, 312–314
41 Piñol-Roma, S. and Dreyfuss, G. (1992) Nature (London) **355**, 730–732
42 Wachter, C., Schatz, G. and Glick, B. S. (1994) Mol. Biol. Cell **5**, 465–474
43 Lithgow, T., Glick, B. S. and Schatz, G. (1995) Trends Biochem. Sci. **20**, 98–101
44 Maccecchini, M. L., Rudin, Y., Blobel, G. and Schatz, G. (1979) Proc. Natl. Acad. Sci. U.S.A **76**, 343–347
45 Reid, G. A. and Schatz, G. (1982) J. Biol. Chem. **257**, 13056–13061
46 Reid, G. A. and Schatz, G. (1982) J. Biol. Chem. **257**, 13062–13067
47 Verner, K. (1993) Trends Biochem. Sci. **18**, 366–371

Received 5 June 1996/1 November 1995; accepted 7 November 1996